JOURNAL OF SOLID STATE CHEMISTRY 113, 355–361 (1994)

# Refined Structure and Properties of the Layered Mott Insulator $BaCoS_2$

G. Jeffrey Snyder,[1] Maria C. Gelabert, and F. J. DiSalvo[2]

*Department of Chemistry, Cornell University, Ithaca, New York 14853*

Received February 7, 1994; accepted March 23, 1994

**$BaCoS_2$ is orthorhombic *Cmma* $a$ = 6.4413(3) Å, $b$ = 6.4926(3) Å, $c$ = 8.9406(3) Å, and is closely related to $BaNiS_2$, which contains Ni–S layers separated by rock salt BaS sheets. Crystals were grown from the melt by slow cooling from 1050 to 950°C. The sulfur atoms in the Co–S layers have very anisotropic thermal displacement parameters, possibly indicating that these sulfurs are actually in a double well potential centered at a high symmetry position in the space group *Cmma*. $BaCoS_2$ is found to be a paramagnetic semiconductor (Mott insulator). The magnetic properties indicate that $BaCoS_2$ undergoes a transformation at 300 K, which is likely due to the onset of antiferromagnetic order.** 

## INTRODUCTION

In the search for new types of superconductors we are trying to emulate the common structural features of the high-temperature copper oxide superconductors with anions other than oxygen, in particular nitrogen or sulfur (1). In order to have extensive mixing of the transition metal $d$ and anion $p$ orbitals at the Fermi level, as seen in the Cu–O systems, the somewhat higher energy sulfur 3$p$ orbitals require that the first row transition metal be to the left of copper, thus having higher energy $d$ orbitals. The sulfides of cobalt are ideal not only because they are usually metallic, but in the +2 oxidation state cobalt has the possibility of being spin ½, which is suggested to be an important characteristic in the copper–oxide superconductors. Since large electropositive cations, such as the heavier alkaline earth metals, may help "enforce" the perovskite-related structure of the copper oxide superconductors, as well as increase the oxidizing power of the oxygen (1), we have chosen a similar strategy and here examine the barium–cobalt–sulfur system.

There are three known barium cobalt sulfides. $Ba_6Co_{25}S_{27}$ is a poor metal with an unusual structure (2) containing cubic clusters of cobalt atoms related to those found in $Co_9S_8$. The semiconducting $Ba_2CoS_3$ is isostructural (3) with $Ba_2FeS_3$, and exhibits quasi-one-dimensional antiferromagnetism, with a $T_{max}$ of 125 K (4). $BaCoS_2$ is very similar in structure to the tetragonal $BaNiS_2$ in which nickel is pentacoordinate to sulfur in a square pyramidal environment (5). The somewhat distorted structure and electronic and magnetic properties of $BaCoS_2$ are the subject of this article.

## EXPERIMENTAL

### *Preparation*

Single-phase polycrystalline $BaCoS_2$ was prepared by reacting a pressed pellet (40,000 psi) containing a molar ratio of reactants, BaS : CoS of 1 : 1. Reactions were carried out in alumina or graphite crucibles sealed in evacuated (10 mTorr) quartz tubes at 950°C. BaS was purchased from Aesar (99.9% metals basis) and CoS was synthesized from the elements (Co, 99.8+%; S, 99.999%). Polycrystalline $BaCoS_2$ was used to grow crystals from the melt. $BaCoS_2$ melts congruently near 1025°C, but at 800°C $BaCoS_2$ decomposes in a peritectoid reaction, where the only crystalline product apparent in X-ray diffraction is $Ba_2CoS_3$. Reheating to 910°C again produces single-phase $BaCoS_2$. The powder is black in contrast to the more brown $Ba_2CoS_3$. The air-stable powder samples were characterized with a Scintag XDS 2000 diffractometer using Cu$K\alpha$ radiation. The contribution of $K\alpha_2$ radiation to the data is stripped using a program supplied by Scintag, so that the resulting pattern is due only to $K\alpha_1$ radiation.

In the course of the study, we found that single phase $BaCoS_2$ was more difficult to obtain with commercially available BaS, presumably due to oxide or hydroxide contamination. Therefore, the polycrystalline samples used for the powder analysis were prepared from BaS synthesized from $BaCO_3$ (Johnson Matthey 99.9% metals basis), following literature methods (6). The pressed pellets of BaS : CoS were heated, in a graphite crucible sealed in an evacuated quartz tube, to 950°C for 60 hr, and quenched in an ice-water bath. The powder patterns of $BaCoS_2$ synthesized from both types of BaS were identical.

[1] Current address: Department of Applied Physics, Stanford University, Stanford, CA 94305.

[2] To whom correspondence should be addressed.



0022-4596/94 $6.00

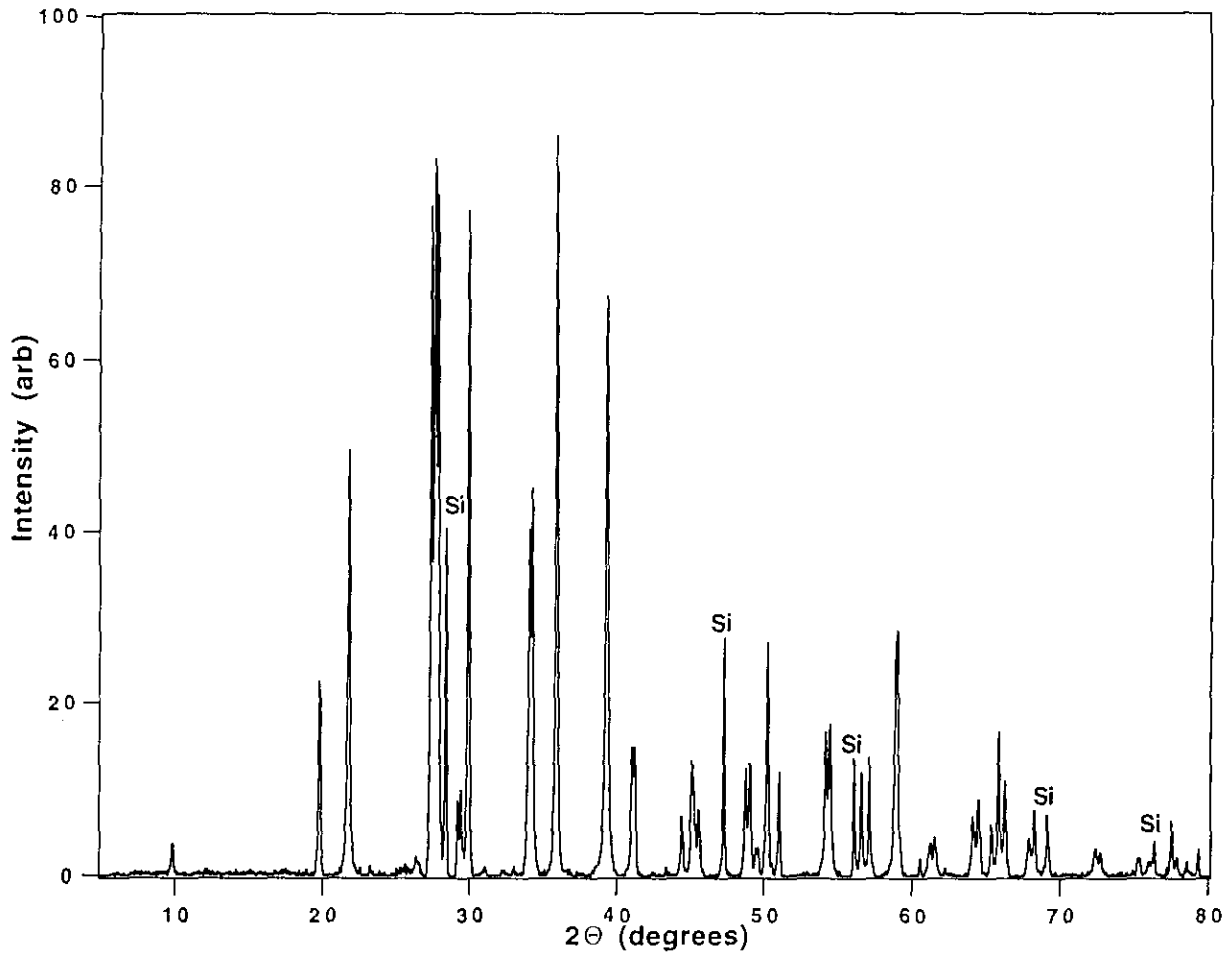


FIG. 1. X-ray powder diffraction pattern of $BaCoS_2$.

Crystals were grown from a melt of polycrystalline $BaCoS_2$, prepared from commercial BaS, by heating to 1050°C and cooling to 950°C at 1°/hr, using a graphite boat sealed in an evacuated quartz tube.

A pellet was used for the resistivity measurements (8 mm diameter, 1.2 mm thick), and was sintered by placing in an alumina crucible, sealing in an evacuated quartz tube, heating at 900°C for 40 hr, and quenching.

*Structure Determination*

The powder pattern of polycrystalline $BaCoS_2$ (Fig. 1) is very similar to the tetragonal $BaNiS_2$ pattern. However, the intense tetragonal *hhl* reflections, emphasized in Fig. 2, are split implying that the gamma angle from the $BaNiS_2$ cell is distorted from 90°. All reflections were indexed using a monoclinic primitive cell, and a Rietveld analysis gives $a_m = b_m = 4.5729(3)$ Å, $c_m = 8.9406(4)$ Å, $\gamma = 90.455(6)°$ (note that in the standard setting $c_m$ and $b_m$ would be switched and the monoclinic angle would be $\beta$). Since $a_m = b_m$, the primitive cell is metrically equivalent to a C-centered orthorhombic Bravais lattice with $a_o = 6.4413(3)$ Å, $b_o = 6.4926(3)$ Å, $c_o = 8.9406(4)$ Å.

Black plate-like crystals of $BaCoS_2$ were selected from the solidified melt of the stoichiometric compound, mounted on a glass fiber with 5-min epoxy, and examined using X-ray diffraction methods. All selected crystals showed multiple peaks during reflection scans and the average lattice parameters (found by the diffractometer) were close to tetragonal, due to *a–b* twinning.

Diffraction data were collected from a large (.3 × .3 × .2 $mm^3$), irregularly shaped crystal. The diffraction peaks were exceptionally broad and non-Gaussian, but were not split as seen in the smaller crystals. The refined orthorhombic cell parameters from this data are $a_o = 6.458$, $b_o = 6.470$, and $c_o = 8.930$ Å. Upon transforming to a monoclinic cell, a 90.11° monoclinic angle is found, significantly closer to 90° (tetragonal $BaNiS_2$ structure) than that of the $BaCoS_2$ powder (90.455°). Because the peaks were asymmetric and broad, the lattice parameters are not considered reliable. Therefore, lattice constants were taken from the powder data.

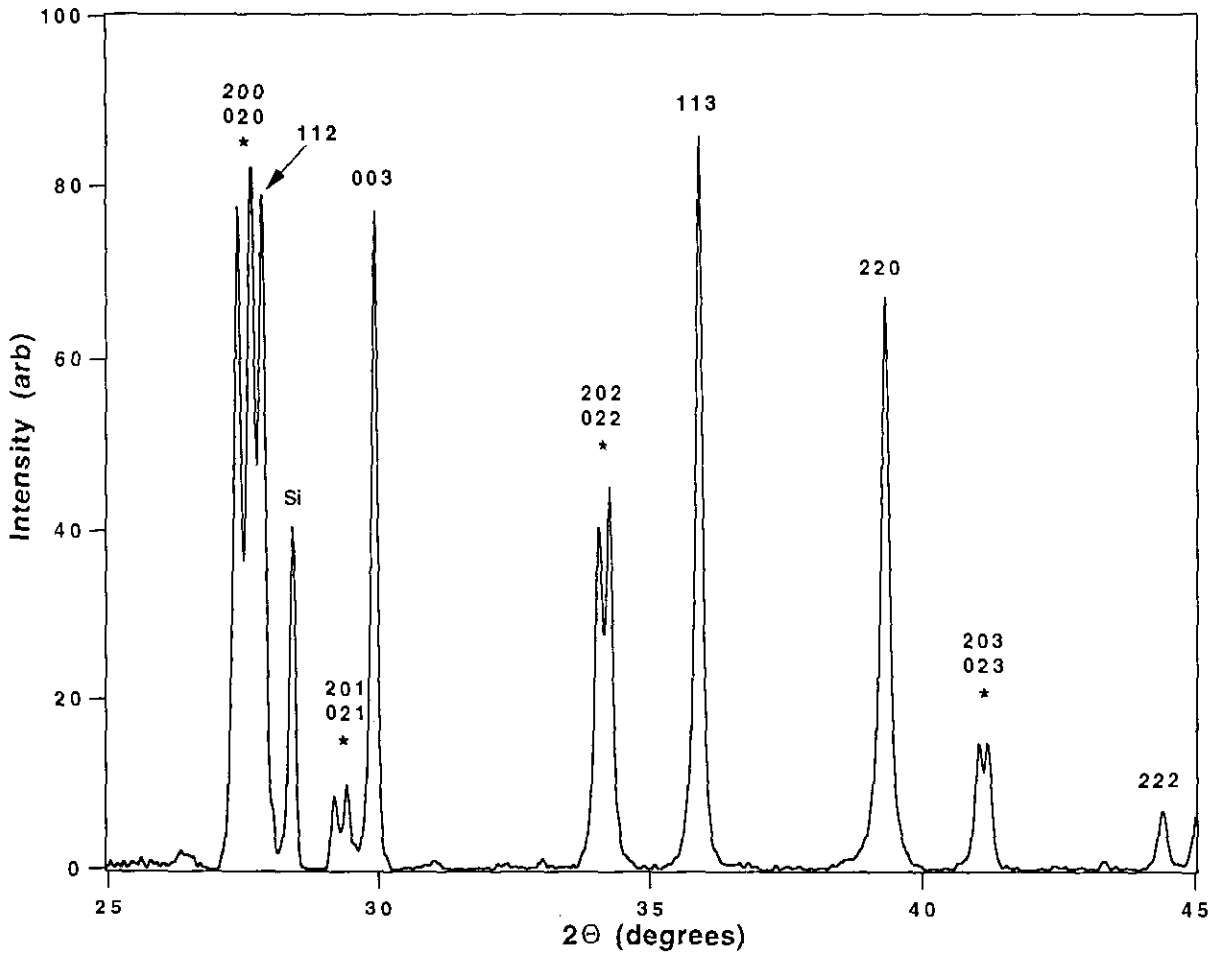


FIG. 2. Enlarged powder pattern, from 25° to 45°. The Miller indices based on the C-centered orthorhombic cell are shown. In the tetragonal $BaNiS_2$ structure, the starred (*) doublets (20l and 02l in the orthorhombic setting) would be singlet 11*l* peaks.

Since the powder diffraction data clearly show that $BaCoS_2$ is not tetragonal, these space groups can be omitted. Data were collected using a C-centered cell, and the systematic absences were consistent with an (*ab*) glide plane. The possible space groups for Laue class *mmm* are then *Cmma* (centrosymmetric) and *Cm2a* (standard setting *Abm2*, noncentrosymmetric). The structure was solved by direct methods. Absorption was corrected empirically (psi scans) with a laminar model, using [001] direction perpendicular to the lamina (XEMP software from Siemens). Better results (lower $R(\sigma)$) were obtained with a higher "take off angle" which removes high absorption reflections along the *ab* plane. In order to minimize a bias by removing reflections, a take off angle of 5° was used in the structure refinement, which removes 10 of 256 independent reflections.

The space group *Cmma* was used for the structure refinement summarized in Table 1. Refinement in *Abm2* or other lower-symmetry space groups did not significantly lower *R* or change the atomic positions. Structure solution and refinement were carried out using SHELXL-93, which is capable of refining twinned crystals. Twinning of the *a*/*b* axes was refined by the method of Pratt, Coyle, and Ibers (7) where the twinning fraction was also refined to 0.45(2), indicating that the crystal had nearly equal twin components. The analytical forms of scattering factors for neutral atoms, as well as corrections for both real and imaginary components of anomalous dispersion, were used as given in the SHELXL-93 software.

The average isotropic displacement parameter for the S(2) atom (the in-plane S) is anomalously large compared to all the other atoms (Table 2). Furthermore, an unusually large anisotropic thermal displacement parameter (Table 3) is found for the S(2) atom along the *b*-axis, which is the direction in which the Co–S sheets are elongated relative to those in $BaNiS_2$.

Moving the S(2) atom off the special position of $y = \frac{1}{2}$ and refining at half occupancy (random distribution between two sites) gives an equally consistent model (*R* is essentially unchanged) but with an average thermal

TABLE 1
Crystal Data and Structure Refinement for $BaCoS_2$

| | |
|---|---|
| Empirical formula | $BaCoS_2$ |
| Formula weight | 260.39 |
| Diffractometer type | Syntex $P2_1$ |
| Monochromator | Graphite |
| Scan type | $\omega - 2\theta$ |
| Temperature | 293(2) K |
| Wavelength | 0.71073 Å |
| Crystal system | Orthorhombic |
| Space group | *Cmma* (No. 67) |
| Unit cell dimensions | $a = 6.4413(3)$ |
| | $b = 6.4926(3)$ |
| | $c = 8.9406(3)$ |
| Volume | 373.91(5) $Å^3$ |
| Z | 4 |
| Density (calculated) | 4.626 $Mg/m^3$ |
| Absorption coefficient | 15.75 $mm^{-1}$ |
| $F(000)$ | 460 |
| Crystal size | .3 × .3 × .2 mm |
| $\theta$ range for data collection | 5.01° to 27.51° |
| Index ranges | $-8 \le h \le 5$, $-8 \le k \le 5$, $-11 \le l \le 11$ |
| Reflections collected | 829 |
| Independent reflections | 246 ($R_{int} = 0.1021$) |
| Refinement method | Full-matrix least-squares on $F^2$ |
| Data/restraints/parameters | 246/0/17 |
| Goodness-of-fit on $F^2$ | 1.244 |
| Final $R$ indices [$I > 2\sigma(I)$] | $R1 = 0.0454$, $wR2 = 0.1306$ |
| $R$ indices (all data) | $R1 = 0.0464$, $wR2 = 0.1317$ |
| Largest diff. peak and hole | 1.734 and −3.449 $eÅ^{-3}$ |

displacement parameter much closer to that of the S(1) atom, and with much more isotropic thermal displacement parameters. Refining in this way for S(2) gives $y = 0.473(5)$ and $U_{eq} = 0.018(5)$ ($Å^2$).

For the S(2) atom to be at this off center position in an ordered way would require either a reduction in symmetry to *Pn* (in the monoclinic setting) or a superstructure. Refinement in *Pn* increases the number of parameters without improving the goodness of fit. Axial photographs of single crystals using both the monoclinic and orthorhombic settings show no indication for an ordered superlattice;

TABLE 2
Atomic Coordinates and Equivalent Isotropic Displacement Parameters [$Å^2 \times 10^3$] for $BaCoS_2$

| | x | y | z | U(eq) |
|---|---|---|---|---|
| Ba | 0 | ¼ | .1981(1) | 14(1) |
| Co | 0 | ¼ | .5932(2) | 18(1) |
| S(1) | 0 | ¼ | .8496(4) | 14(1) |
| S(2) | ¼ | ½ | ½ | 31(1) |

*Note.* $U(eq)$ is defined one third of the trace of the orthogonalized $U_{ij}$ tensor.

TABLE 3
Anisotropic Displacement Parameters ($Å^2 \times 10^3$) for $BaCoS_2$

| | $U_{11}$ | $U_{22}$ | $U_{33}$ | $U_{23} = U_{13} = U_{12}$ |
|---|---|---|---|---|
| Ba | 19(2) | 11(2) | 13(1) | 0 |
| Co | 23(3) | 16(2) | 14(1) | 0 |
| S(1) | 21(3) | 9(2) | 11(2) | 0 |
| S(2) | 13(2) | 62(4) | 17(1) | 0 |

*Note.* The anisotropic displacement factor exponent takes the form $-2\pi^2[(ha^*)^2U_{11} + \cdots + 2hka^*b^*U_{12}]$.

however, such reflections might have been too weak to be observed by this method. A collaborative TEM diffraction study is planned to search for a potential superlattice (8). Even if these S(2) atoms were off center in an ordered way, they would only be 0.35(6) Å from an equivalent unoccupied site, well within the range due to thermal movement at room temperature. Since we cannot unambiguously determine the nature of this anomaly, we report the S(2) atom at full occupancy in the high-symmetry special position and space group as *Cmma*. A recent independent study on an apparently untwinned crystal essentially confirms these results (9).

### *Electrical Resistivity*

Four probe resistivity measurements were performed at 23 Hz by lock-in detection. The contacts were shown to be ohmic by the linearity of the I–V characteristic.

Indium metal contacts (made at four points on the edge of the pellet) were used for the variable-temperature study. Using the method of Van der Pauw (10) for flat samples, the room temperature resistivity of the pellet was 4.8 ohm cm. Resistivity versus temperature from 390 to 150 K is shown in Fig. 3.

The resistivity of a small single crystal (.23 × .13 × .09 $mm^3$) was also examined in order to show that the polycrystalline data were characteristic of the phase and not of intergrain resistance or other extrinsic effects. The middle two contacts used for voltage measurements were 0.12 mm apart. Using four contacts, made with silver paint, the resistivity of the single crystal was 1.5(3) ohm cm at room temperature, indicating that the pellet used for resistivity measurements was well sintered. The large estimated error in resistivity arises from the large size of the contacts relative to their separation. The resistivity of the crystal had a similar temperature dependence as the polycrystalline pellet, but the contacts were not as reliable upon thermal cycling.

### *Magnetic Susceptibility*

The Faraday technique was used to measure the magnetic susceptibility of a 104.4-mg powder sample of

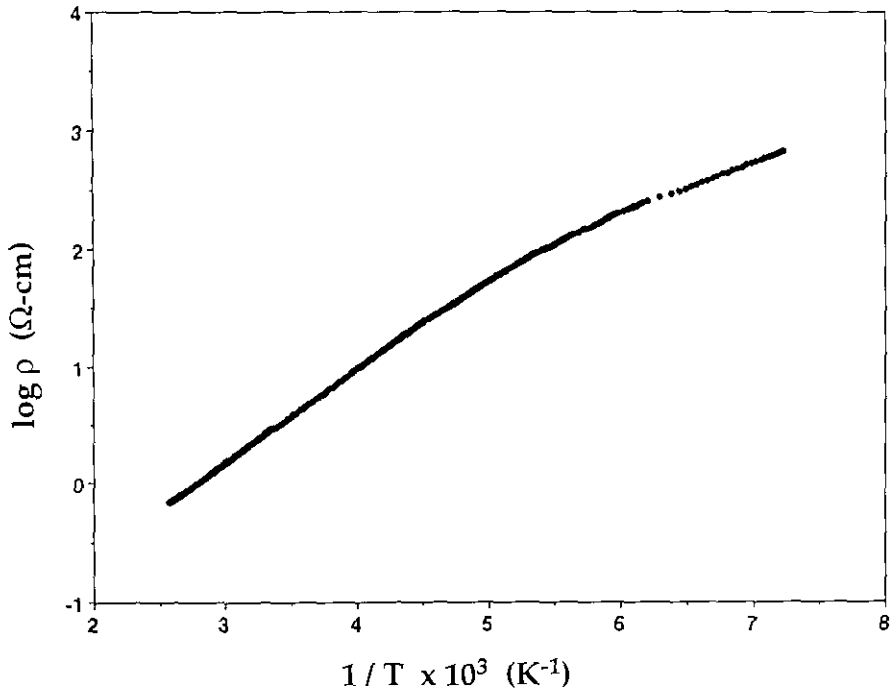


FIG. 3. Log resistivity as a function of inverse temperature.

$BaCoS_2$ as a function of temperature, in a previously calibrated system (11). The susceptibility was measured as a function of the applied field, and found to be essentially field independent, indicating an insignificant contamination of ferromagnetic impurity. The measured magnetic susceptibility, shown in Fig. 4, shows a break in slope at 300 K and a small paramagnetic impurity contribution that dominates the low-temperature susceptibility. Features around 60 K, attributed to a small oxygen gas impurity in the He heat exchange gas in the apparatus, were removed from the data.

## RESULTS AND DISCUSSION

### *Structure Description*

$BaCoS_2$ has a structure very different from the two other known barium–cobalt–sulfides. Metallic $Ba_6Co_{25}S_{27}$ is comprised of cubic $Co_8S_6$ clusters containing significant Co–Co bonding, connected via an octahedrally coordinated cobalt atom. Semiconducting $Ba_2CoS_3$, however, consists of chains of corner sharing $CoS_4$ tetrahedra with no metal–metal bonding but with strong one-dimensional antiferromagnetic coupling through the S atoms. $BaCoS_2$ is the only layered barium–cobalt–sulfide, and contains an unusual five-coordinate cobalt atom.

$BaCoS_2$, as in $BaNiS_2$, contains layers of CoS sandwiched between two rock-salt layers of BaS. The cobalt atoms are alternately 0.83 Å above and below the layer plane with additional coordination to one sulfur atom in the BaS layer. Thus the cobalt is five-coordinate forming nearly square $CoS_5$ pyramids. As shown in Fig. 5, these pyramids form infinite $[CoSS_{4/4}]_n^{2n-}$ sheets with the apical S(1) atoms alternately up and down. The Ba atoms are nine-coordinate with four S(2) neighbors from the adjacent CoS layer, four S(1) atoms from its own layer, and one S(1) atom from the neighboring BaS layer.

$BaCoS_2$ differs from $BaNiS_2$ in that the fourfold tetragonal symmetry of $BaNiS_2$ is reduced to twofold orthorhombic. The size of the primitive cells are similar and the number of atoms in the asymmetric unit in both phases is the same, only the local symmetry of the atoms has changed.

The symmetry breaking is probably best described in terms of the monoclinic angle $\gamma$ in the primitive cell with $a = b = 4.5729(3)$ Å. In the tetragonal $BaNiS_2$ cell $\gamma$ is of course 90° while in pure $BaCoS_2$ $\gamma = 90.455(6)°$. It has also been reported that the systems $BaCo_{1-x}Ni_xS_2$, have $\gamma = 90°$ even with as little as 10% Ni (12). A temperature-dependent X-ray study to search for crystallographic transitions is underway (8).

The Mott insulator character is consistent with the relatively large unit cell volume of $BaCoS_2$. The primitive cell volume is 7.2% larger than that of $BaNiS_2$, and decreases rapidly with nickel substitution (13) as the system becomes metallic. A comparison with binary sulfides further demonstrates this point with the transition metal atoms

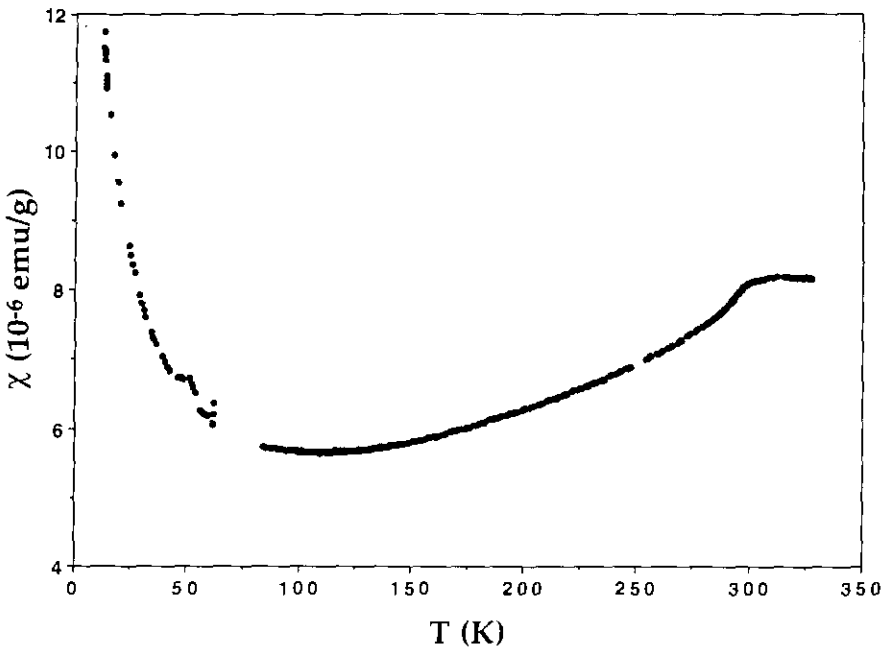


FIG. 4. Magnetic susceptibility as a function of temperature.

reversed. Insulating $NiS_2$ has a cell 9% larger than the metallic $CoS_2$.

The Ba–S distances in $BaCoS_2$ (3.1 to 3.5 Å, Table 4) compare well with those of BaS (3.19 Å) and the average values in the other ternary compounds, $Ba_6Co_{25}S_{27}$ (3.22 Å) and $Ba_2CoS_3$ (3.20 Å). The five-coordinate Co–S(1) distance in $BaCoS_2$ of 2.29 Å is between the distances found for four-coordinate Co in $Co_3S_4$ and $Co_9S_8$ which range from 2.18 to 2.24 Å, and the six-coordinate Co in CoS and $Co_9S_8$ which are about 2.35 Å.

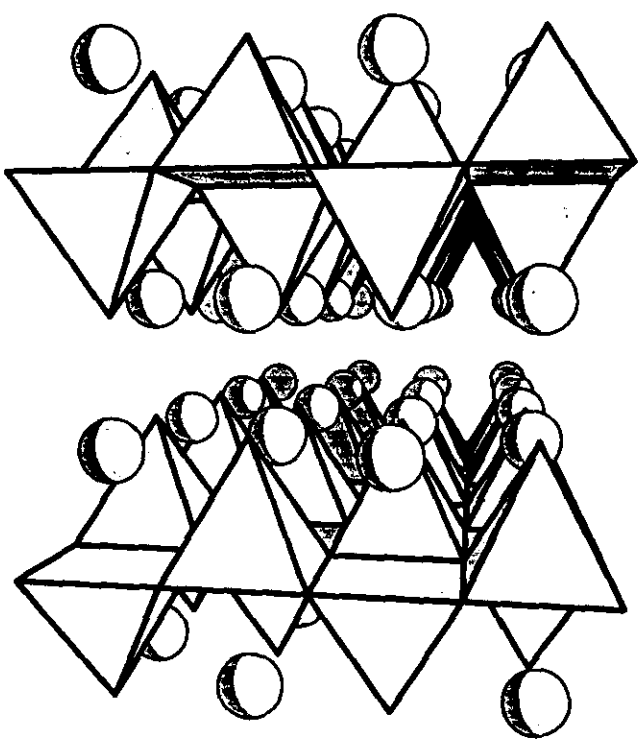

FIG. 5. Structure of $BaCoS_2$, where the spheres represent Ba atoms and the square pyramids represent $CoS_5$ polyhedra.

The Co–S(2) bond distance of 2.435 Å is a surprising 6% longer than the Co–S(1) distance, and is longer than in any known Co–S or Ba–Co–S phase. In comparison, the Ni–S(2) distance in $BaNiS_2$ is only 1% longer than the Ni–S(1) distance. Using the model with the S(2) atom off the $y = \frac{1}{2}$ position gives the closest Co–S(2) distance of 2.32(2) Å, which is the expected 1% longer. This may indicate that a double well model (the two positions are only 0.35(6) Å apart), or an ordered variant thereof, of the S(2) position is actually a better description of the structure.

*Physical Properties*

Charge consistent extended Hückel calculations predict $BaCoS_2$ to have extensive S(3*p*)–Co(3*d*) overlap at the Fermi level in a relatively narrow band, with the Co

TABLE 4
Selected Bond Lengths (Å) and Angles (degrees) for $BaCoS_2$

| | | | | | |
|---|---|---|---|---|---|
| Co–S(1) | ×1 | 2.292(3) | Co–S(2) | ×4 | 2.434(1) |
| Ba–S(1) | ×1 | 3.116(4) | Ba–S(1) | ×2 | 3.249(1) |
| Ba–S(1) | ×2 | 3.274(1) | Ba–S(2) | ×4 | 3.537(1) |
| S(1)–Co–S(2) | | 110.02(4) | S(2)–Co–S(2) | | 82.86(3) |
| S(2)–Co–S(2) | | 83.67(3) | S(2)–Co–S(2) | | 139.95(8) |

$3d_{z^2}$ and $3d_{x^2-y^2}$ ($z$ along $c$) antibonding orbitals partially filled, and hence metallic behavior (14). However, the resistivity curve (Fig. 3) shows that $BaCoS_2$ is a thermally activated semiconductor. This sample at room temperature has an activation energy of 0.17 eV, most likely due to extrinsic impurities or defects, rather than indicating an intrinsic band gap of 0.34 eV.

The large room-temperature paramagnetic susceptibility, assuming a simple Curie law, requires an average spin of about 0.7 per cobalt atom. This implies that the cobalt atoms have magnetic moments due to localized electrons consistent with our view of $BaCoS_2$ as a Mott insulator. The cobalt is probably not simply a spin $\frac{1}{2}$ ion, but high-temperature data are needed to unambiguously determine the magnitude of the spin.

Assuming that the low-temperature Curie susceptibility is due to paramagnetic impurities, and further assuming that these are mostly due to Fe, we calculate an impurity concentration of about 0.5%. This is somewhat higher than expected for the stated Co purity of 99.8%, but within the realm of possibility.

The gradual drop in susceptibility below 300 K is indicative of a second order phase transition at this temperature. Since the electrical conductivity of $BaCoS_2$ does not noticeably change at this temperature, the transition is most likely magnetic in origin. The nearest Co–Co distance within a sheet is 3.6 Å, while the nearest interlayer Co–Co distance is more than 8 Å, leading one to expect primarily two-dimensional exchange between Co local moments. The exact nature of the exchange is presently uncertain, and will be the subject of future studies. The room-temperature susceptibility of $BaCo_{1-x}Ni_xS_2$ drops rapidly and the transition apparently broadens and moves to lower temperature with increasing nickel substitution (12).

## CONCLUSIONS

$BaCoS_2$ has a weakly distorted structure very similar to that of $BaNiS_2$. Since it must be quenched from high temperatures, we presume that it is metastable at room temperature. The compound is a Mott insulator with layers structurally related to the high-temperature copper oxide superconductors. Indeed, $BaCoS_2$ satisfies the proposed criteria (15) for "finding new superconductors": (1) the barium sites are suitable for doping to introduce itinerant charge carriers without introducing disorder into the Co–S layers; (2) the system is near a metal-insulator Mott transition, as proven in the $BaCo_{1-x}Ni_xS_2$ system; (3) the cobalt spin is close to $\frac{1}{2}$ in the paramagnetic state, and seems to order antiferromagnetically; (4) the cobalt $d$ antibonding orbitals are extensively mixed with the sulfur $p$ orbitals at the Fermi level, with no extended metal–metal bonding; and (5) $BaCoS_2$ contains two-dimensional Co–S sheets.

## ACKNOWLEDGMENTS

We thank Michael Badding, Richard Dronskowski, Nate Brese, Andrew A. Guzzelian, Chris Briggs, and Abby Wizansky for discussions and assistance on this project. G. J. S. is grateful for the use of equipment at the M.P.I. Stuttgart, and the financial support by the R.E.U. program sponsored by the Materials Science Center at Cornell, through Grant NSF-DMR88-8516616, the Office of Naval Research, and the Hertz foundation.

## REFERENCES

1. F. J. DiSalvo, "Chemistry of High-Temperature Superconductors" (D. L. Nelson, M. S. Whittingham, and T. F. George, Eds.), p. 49. American Chemical Society, Washington, D.C., 1987.
2. G. J. Snyder, M. E. Badding, and F. J. DiSalvo, *Inorg. Chem.* **31,** 2107 (1992).
3. H. Y. Hong and H. Steinfink, *J. Solid State Chem.* **5,** 93 (1972).
4. N. Nakayama, K. Kosuge, S. Kachi, T. Shinjo, and T. Takada, *J. Solid State Chem.* **33,** 351 (1980).
5. I. E. Grey and H. Steinfink, *J. Am. Chem. Soc.* **92,** 5093 (1970).
6. G. Brauer (Ed.), "Handbook of Preparative Inorganic Chemistry," 2nd ed., p. 938. Academic Press, New York, 1963.
7. C. S. Pratt, B. A. Coyle, and J. A. Ibers, *J. Chem. Soc. (A)* **12,** 2146 (1971).
8. In collaboration with R. Brec and co-workers at the Institut des Materiaux de Nantes, France.
9. N. C. Baenziger, L. Grout, L. S. Martinson, and J. W. Schweitzer, *Acta Cryst. C,* in press.
10. L. J. Van der Pauw, *Philips Res. Rep.* **13,** 1 (1958).
11. J. Vassiliou, M. Hornbostel, R. Ziebarth, and F. J. DiSalvo, *J. Solid State Chem.* **81,** 208 (1989).
12. L. S. Martinson, J. W. Schweitzer, and N. C. Baenziger, *Phys. Rev. Lett.* **71**(1), 125 (1993).
13. L. S. Martinson, private communication.
14. Richard Dronkowski, MPI Stuttgart.
15. T. H. Geballe, *Science* **259,** 1550 (1993).